

Journal of Materials Chemistry C

Accepted Manuscript

This article can be cited before page numbers have been issued, to do this please use: J. Hong, W. Chien, T. Chen and S. Deng, *J. Mater. Chem. C*, 2013, DOI: 10.1039/C3TC31592D.



This is an *Accepted Manuscript*, which has been through the RSC Publishing peer review process and has been accepted for publication.

Accepted Manuscripts are published online shortly after acceptance, which is prior to technical editing, formatting and proof reading. This free service from RSC Publishing allows authors to make their results available to the community, in citable form, before publication of the edited article. This *Accepted Manuscript* will be replaced by the edited and formatted *Advance Article* as soon as this is available.

To cite this manuscript please use its permanent Digital Object Identifier (DOI®), which is identical for all formats of publication.

More information about *Accepted Manuscripts* can be found in the [Information for Authors](#).

Please note that technical editing may introduce minor changes to the text and/or graphics contained in the manuscript submitted by the author(s) which may alter content, and that the standard [Terms & Conditions](#) and the [ethical guidelines](#) that apply to the journal are still applicable. In no event shall the RSC be held responsible for any errors or omissions in these *Accepted Manuscript* manuscripts or any consequences arising from the use of any information contained in them.

Aggregation-Enhanced Emission in Fluorophores Containing Pyridine and Triphenylamine Terminals: Restricted Molecular Rotation and Hydrogen-bond Interaction

Shiang-Lin Deng, Tai-Lin Chen, Wei-Lun Chien and Jin-Long Hong*

*Department of Materials and Optoelectronic Science
National Sun Yat-Sen University
Kaohsiung 804214, Taiwan*

Restriction on molecular rotation of fluorophores reduces non-radiative decay channels and promotes strong fluorescence due to aggregation-enhanced emission (AEE) behavior. To evaluate the important role of restricted molecular rotation on AEE behavior, tetraphenylthiophene (TP) derivatives with two pyridine (Py) or two triphenylamine (TPA) terminals were synthesized and characterized to be AEE-active fluorophores. Because of the efficient hindered molecular rotation of the larger TPA terminals, TP-2TPA emitted with higher emission efficiency than TP-2Py with smaller Py terminals. In addition, Py and TPA terminals can serve as hydrogen-bond (H-bond) accepting groups to bind with H-bond donating hydroxyl groups in poly(vinyl phenol) (PVPh) and poly(vinyl alcohol) (PVA) to further reinforce rotational restriction on the TP-2Py and TP-2PTA fluorophores. TP-2Py and TP-2PTA were therefore blended with PVPh and PVA and the emissive properties of the resultant blends were characterized and compared with the unblended TP-2Py and TP-2PTA to emphasize the role of H-bond on restricted molecular rotation.

Introduction

Conventional planar, disk-like organic fluorophores exhibit high fluorescence in dilute solutions but suffer from detrimental aggregation-caused quenching (ACQ) in concentrated solutions and solid states. The fluorescence quenching of conventional fluorophores in the solid state greatly limits their real-world application. In contrast, 1-methyl-1,2,3,4,5-pentaphenylsilole, the first fluorophore with aggregation-induced emission (AIE) property, has the unusual behavior that it emitted strongly in the solution aggregated or in the solid state despite its non-emissive dilute solution state.¹ The AIE effect of silole derivatives was attributed to the restricted intramolecular rotation (RIR) of the phenyl peripheries²⁻⁵ against the central silole core in the aggregate state. It was rationalized that effective RIR in the aggregated states of AIE-active fluorophores reduces the possible nonradiative decay channels and leads to enhanced radiative recombination of the excited state and the strong fluorescence. In view that RIR is the main mechanism responsible for AIE activity, substituent with large molecular size was covalently-linked to AIE-active centers (e.g. silole⁶ and tetraphenylethene⁷) to induce hindered rotation and the desired emission enhancement. Since the first discovery of the silole system, lots of organic and polymeric materials⁸⁻¹⁵ with AIE or aggregation-enhanced emission (AEE) properties have been prepared and characterized.

Since physical interaction forces can be used to reinforce restriction on molecular rotation, several reports had been focused on evaluating the relationship between hydrogen-bond (H-bond) and molecular rotation of AIE (or AEE) active materials. A fluorenone-derivative of 2,7-bis(4-(*tert*-butylthio)phenyl)-fluorenone (DSFO)¹⁶ was reported to have enhanced excimer emissions due to intermolecular H-bonds. The dimer structure of DSFO was locked by intermolecular H-bonds and the corresponding excimer emission underwent fewer non-radiative decay pathways.

The salicylideneaniline (SA)¹⁷ compound formed gel in certain organic solvents and the resultant gel solution was reported to have a fluorescent quantum yield (Φ_F) 600 times higher than that of the homogeneous solution. The AEE property is ascribed to the formation of *J*-aggregates and the inhibition of molecular rotation by H-bond interactions in the viscous gel. Other systems relating compounds with hydrazine¹⁸, benzoxazole¹⁹, acrylamido²⁰ and naphthalide²¹ functions were also found to exhibit enhanced emission in the gelled states promoted by H-bond interactions. Poly(fluorene-*alt*-naphthol)²² previously prepared in our laboratory was also found to exhibit AEE properties due to the restricted molecular rotation promoted by inter and intrachain H-bonds among the inherent hydroxyl side groups. The restricted molecular rotation of PFN can be further enhanced by blending it with different amounts of poly(*N*-vinyl pyrrolidone)²³ (PVR). Through the facile intermolecular H-bond interactions between PFN and PVR, a PFN/PVR blend with small amounts (2.3 wt%) of PFN can emit with a high Φ_F value of 93%. Blend using H-bond interactions were also conducted in small molecule system. An AEE-active fluorophore with pyridine terminals was mixed with either small-mass bisphenol A or polymeric poly(vinyl phenol)²⁴ to generate pseudo-linear or pseudo-crosslinked blends with higher emission intensity compared to the starting fluorophore. Use of H-bond interactions to lock the molecular rotations of organic and polymeric fluorophores was therefore illustrated by the above examples and with effective restriction on molecular rotation, the AEE-active fluorophores possess a beneficial strong emission in the solid state, which facilitates their solid-state applications (e.g. as a light-emitting layer in an organic light-emitting diode (OLED)). Under the premise that the emission performance can be maintained or enhanced, blending the valuable AEE-active fluorophores with other inexpensive, commercialized materials provides alternative routes to cut down the costs in practical applications.

In this study, the idea of using large substituent and H-bond interaction to reinforce restricted molecular rotation was further tested on new AEE-active fluorophores. To execute the idea, a former AEE-active tetraphenylthiophene (TP)²⁵ fluorophore was used as the main structural center to link with either pyridine (Py) or two triphenylamino (TPA) terminals via double bond (Scheme 1). The AEE-active fluorophores of TP-2Py and TP-2PTA differ in the size of terminal groups used and with the large TPA terminals, TP-2PTA emitted strongly with a high solid Φ_F value of 80% as compared to 50% obtained for TP-2Py with smaller Py terminals. This result is correlated with the size effect on restricted molecular rotation. In addition, we intended to use Py and TPA terminals, as the potential H-bond acceptors, in the respective TP-2Py and TP-2TPA to H-bond to hydroxyl groups in poly(vinyl phenol) (PVPh) and poly(vinyl alcohol) (PVA) (Scheme 2) to reinforce restriction on molecular rotation. However, unexpected fluorescence reduction was found when TP-2Py was blended with PVPh, which is distinguished from the enhanced emissions observed in blends of TP-2Py/PVA, TP-2PTA/PVPh and TP-2PTA/PVA. The varied fluorescence responses in terms of potential side reaction and degree of molecular rotation are therefore the focuses of this research.

Results and Discussion

Synthesis

As illustrated in Scheme 1, the fluorescent molecules of TP-2Py and TP-2TPA were synthesized from the Heck-coupling reaction, with which reaction between 4-vinylpyridine (V-Py) and 2,5-bis(4-bromophenyl)-3,4-diphenylthiophene (TP-2Br) yielded TP-2Py whereas reaction between TP-2Br and *N,N*-diphenyl-4-vinylaniline (V-TPA) obtained TP-2TPA. Beforehand, the key intermediate of TP-2Br needed to be prepared from bromination of TP^{26,27} in the presence of bromine/FeCl₃. For

preparation of TP-2PTA, the required compound of V-TPA was synthesized from a two-step reaction scheme, with the first step formylation of triphenylamine (TPA) to obtain F-TPA and the following Wittig reaction of F-TPA in the presence of $\text{PPh}_3\text{CH}_3\text{Br} / t\text{-BuOK}$. Chemical structures of all intermediates and products were confirmed from the corresponding ^1H NMR (Fig. S1-S5) and elemental analysis. The double bonds in TP-2Py and TP-2TPA are all *trans* in geometry as judged by the resolved coupling constants ($J_{trans} > 15$ Hz) of the alkene protons in the corresponding ^1H NMR spectra. Both products of TP-2Py and TP-2PTA are amorphous materials with glass transition temperatures (T_g s) at 102 and 140 °C (Fig. S6-S7), respectively. The higher molar mass of TP-2TPA contributes to its higher T_g as compared to TP-2Py molecule with lower molar mass.

Aggregation-enhanced emission (AEE) behavior of TP-2Py and TP-2TPA

Effect of concentration on TP-2Py and TP-2TPA were described in the unnormalized solution PL emission spectra in Fig. 1A and 1B, respectively. Both solution systems exhibited the continuous gain of the emission intensity as concentration of the fluorophore in THF was increased from 10^{-6} to 10^{-3} M. Whereas solution thickening often weakens (or quenches) fluorophore's emission, the solutions of TP-2Py and TP-2TPA become more emissive with higher concentration and this concentration-enhanced emission is typical of AEE-active fluorophores. For TP-2Py (Fig.1A), solution of very low fluorophore content (10^{-6} M) is weakly-emissive but increasing concentration from 10^{-5} to 10^{-3} M, two emission peaks at 452 and 481 nm started to emerge and gained their intensity with increasing concentration. These two emissions should be attributed to varied vibronic electronic states instead of monomer and aggregate emissions based on the small spacing ($1389\text{ cm}^{-1} < 1400\text{ cm}^{-1}$)²⁸ between these two emission peaks and the proportional increase of both bands with

increasing concentration. In case of preferable aggregation in more concentrated solution, we would expect an inevitable increase on the long-wavelength aggregate emission band. The two-peak pattern however disappeared and was replaced by a broad peak at 500 nm in the spectrum of solid TP-2Py. Compared to solution sample, red-shift of the emission peak in the solid TP-2Py indicates a more extended conformation existing in the solid TP-2Py. For TP-2PTA, only one broad emission peak at 500 nm was resolved (Fig. 1B). The continuous emission gain with increasing concentration also suggests that TP-2PTA is an AEE-active fluorophore. Compared to TP-2Py under the same concentration, TP-2PTA emitted with larger intensity.

The AEE effect was also characterized by the PL emission spectra of TP-2Py and TP-2TPA in THF/hexane solvent/poor solvent pair. Primary evaluation indicated that hexane is a poor solvent for both fluorophores, the inclusion of hexane in the homogeneous fluorophore solutions in THF induced molecular aggregations and the corresponding spectral responses can be used to study the effect of aggregation on fluorescence behavior. The solution emission intensities for TP-2Py and TP-2TPA (Fig. 2) are all increased with increasing hexane content, which fits the characteristics of AEE behavior that aggregation due to inclusion of poor solvent leads to emission enhancement. For TP-2Py, the proportional increase of both emission bands once again confirms the vibronic nature of these two bands. Development of aggregated structure of TP-2Py upon hexane inclusion can be evaluated from dynamic light scattering (DLS) (Fig. S8). Aggregated particles of TP-2Py in the 30 vol%-hexane solution possess an average hydrodynamic diameter (D_h) of 610 nm whereas the 60 and 80 vol%-hexane solutions contains nanoparticles with smaller D_h values of 390 and 110 nm, respectively. Addition of hexane clearly reduced the particle size; therefore, the congested environment in the shrunk nanoparticles is effective in imposing rotational restriction on the fluorophores; thus, leading to enhanced

emission of the aggregated nanoparticles.

Restricted molecular rotations of TP-2Py and TP-2TPA

It is known that rotational energy relaxation can non-radiatively deactivate the excited specie and consequently weaken (or quench) the fluorescence. In the dilute solution state, the excited species are easily deactivated through molecular collisions with the surrounding solvent molecules, thus making the fluorescent molecules non-emissive. In the solid aggregates, molecular motions are considerably frozen and consequently, the possibility of non-radiative decay channels are largely reduced and the radiative process acts to result in emission enhancement. The effectiveness of the restriction forces determines the resolved fluorescence intensity of the AIE or AEE-active fluorophores. Under the same solution conditions (cf. Fig. 1 and 2), TP-2TPA all have higher emission efficiency than TP-2Py and the solid TP-2TPA also has a higher quantum yield ($\Phi_F = 80\%$, Table 1) than that ($= 50\%$) of the solid TP-2Py. This result suggests that molecular rotation of TP-2PTA should be more effectively restricted in comparison to TP-2Py.

Since molecular rotations can be thermally activated, the emission intensity at different temperatures is therefore useful for evaluating relative degree of rotational restriction on the fluorophores. It is known that cooling increases the viscosity and friction of the solution mixtures and thereby, hampers the non-radiative decay process detrimental for fluorescence. We therefore measured the emission spectra of TP-2Py and TP-2TPA in THF at reduced temperatures from 293 to 153 K. The emission spectra at reduced temperatures (Fig. 3) showed that both samples emitted with increasing intensity as the system temperature was decreased; however, a less pronounced temperature effect was resolved for TP-2TPA as compared to the significant emission enhancement observed for TP-2Py. Through the whole cooling

cycle, the emission intensity of TP-2Py became twice of the starting emission band at room temperature, which is in distinction to the minor (< 10%) emission enhancement observed for TP-2TPA. The less pronounced temperature effect on TP-2PTA should be attributed to its higher rotation energy barrier (more effective restriction on molecular rotation) as compared to TP-2Py. Molecular rotation of TP-2PTA is said to be effectively prohibited and decreasing temperature did not help much on hampering the molecular motion. With lower rotation barrier, TP-2Py molecules in dilute solution rotates freely at room temperature and upon cooling, the involved molecular rotations can be efficiently prohibited in the frozen media, which is particularly true when the temperature was lowered to below melting point (= 258 K) of THF, to result in large emission enhancements.

To demonstrate that restricted molecular rotation is the key factor leading to the varied emission responses of TP-2Py and TP-2TPA toward cooling, computations on rotation barriers were conducted by Molecular Studio (*MS*) software. The resultant single-molecule conformers of TP-2Py and TP-2TPA with minimum energy were given at top of Fig. 4, which illustrates the fundamental difference between the C2-substituents of both molecules. The two (A and B) rings in the C2-substituent of TP-2Py are tilted to each other to adopt a non-coplanar arrangement, which is in wide distinction to the coplanar C and D rings in the C2-substituent of TP-2PTA. The C2-substituent should be responsible for the observed fluorescence and its non-coplanar geometry may contribute to the observed two-band emission pattern. On the contrast, more extensive electron delocalization over the more coplanar C2-substituent of TP-2TPA may homogenize the energy levels of the excited electronic state, leading to the broad one-band emission pattern at longer wavelengths than the two bands in TP-2Py.

Rotation barrier is considered to be the average energy required to rotate the

single bond (bond 1) connecting the C2-substituent and the central thiophene ring from the equilibrium position of the minimum-energy conformer to other conformers with rotation angles deviated from the equilibrium one. The calculated energy barrier was plotted against the rotation angle at the bottom of Fig. 4. For TP-2Py, the maximum energy barrier (< 300 Kcal/mol) occurred at a rotation angle of 160°; in contrast, the calculated energy barrier of TP-2PTA arose quickly as the rotation angle exceeded ~ 140 ° and reached a maximum value of 600 Kcal/mol at an angle of 180°. Supposedly, this result is directly related to the large steric repulsion forces between the bulky C-2 substituent and the central thiophen ring. Rotation of the bulky C-2 substituent of TP-2TPA is surely a more difficult task than rotating the smaller C-2 substituent of TP-2Py, which is considered to be responsible for the more efficient emission of TP-2PTA when compared to TP-2Py.

H-bond interactions of TP-2Py and TP-2TPA

With the respect that the terminal Py and TPA groups are H-bond acceptors, the AEE-active TP-2Py and TP-2TPA were therefore reacted with H-bond donating hydroxyl groups in poly(vinyl phenol) (PVPh) and poly(vinyl alcohol) (PVA) for the sake of reinforcing rotational restriction. To maximize restriction forces, polymeric poly(vinyl phenol) (PVPh) and poly(vinyl alcohol) (PVA) with hydroxyl function equivalent to Py and TPA terminals in the respective TP-2Py and TP-2TPA fluorophores were used. With the mutual H-bond interaction, molecular rotation of the C2-substituents can be effectively restricted to result in better emission efficiency than pure TP-2Py and TP-2TPA without polymer additives.

Primarily, the solid TP-2Py/PVPh and TP-2TPA/PVPh blends containing equal amounts of H-bond donating and accepting groups were prepared from the homogeneous fluorophor/PVPh solutions in THF. Dilute solutions were virtually

homogeneous but during the slow evaporation of THF solvent certain amounts of blended products, presumably with physical crosslinked network structure, precipitated from the solutions.

The mutual H-bond interactions between polymers and TP-2Py (or TP-2PTA) should change the chain dimensions of the polymers in THF. Once H-bonded to polymeric PVA and PVPh, TP-2Py and TP-2PTA molecules should serve as anchoring junctions in between hydroxyl groups of functions of PVA and PVPh and therefore, they will function to shorten the intra- and inter-chain distances of the polymers to result in aggregates smaller than the pure polymers. The hypothetical size variations can be conveniently evaluated from DLS analysis (Fig. S9) on the dilute (10^{-5} M) solutions of pure PVA, PVPh, TP-2Py/PVA and TP-2PTA/PVPh mixtures in THF. Chain segments of pure PVA and PVPh formed large aggregates with the detected D_h s $> 1 \mu\text{m}$ and as expected, preferable H-bond interactions between fluorophores and polymers considerably shrunk the aggregated particles (with the detected D_h s smaller than 500 nm). Variations on the sizes of the aggregates can be used to demonstrate the presence of H-bond interactions between Py terminals of TP-2Py (or TPA terminals of TP-2PTA) and hydroxyl functions of polymers.

After complete solvent removal, the resultant solid TP-2Py/PVPh and TP-2PTA/PVPh blends all exhibited emission at the same wavelengths as the pure TP-2Py and TP-2PTA (Fig. 5A). However, the solid TP-2Py/PVPh blend showed an unexpected reduction on the emission intensity (Fig. 5A) when compared to the pure TP-2Py itself, this result is quite different from the TP-2PTA/PVPh blend (Fig. 5B) that PVPh in this case actually functioned as rotational restrictor to result in better emission efficiency than the unblended TP-2PTA itself.

Long chain polymers should impose effective restriction on molecular mobility of the small-mass TP-2Py and TP-2PTA; however, the multiple hydroxyl pendant

groups along the polymer chain of PVPh and PVA will generate lots of intermolecular physical junction points when H-bonded to TP-2Py and TP-2PTA molecules in the solution state and the resultant crosslinked networks in the solution should prevent the hydroxyl functions in polymer chains from complete H-bonding. Blend systems were prepared from mixing of both components in THF solvent. To avoid the premature precipitation of the crosslinked products, all solution mixtures were agitated vigorously during the solution mixing step; however, visible precipitates still occurred during the mixing process. After removal of THF solvent, the resultant solid blends were sent for spectral measurement immediately.

Incorporation of PVPh in the blends caused different emission responses between TP-2Py and TP-2PTA (Fig. 5). Obviously, emission intensity was drastically reduced by PVPh in the blend; on the contrary, further emission enhancement was observed in TP-2PTA system. What is the origin for the varied responses toward PVPh addition? It should relate to the potential acid-base reaction, which is less probable in TP-2TPA/PVPh system, between the weakly-alkaline Py terminals of TP-2Py and the acidic phenolic pendant groups of PVPh. The protonated TPA (TPAH^+X^-) is a highly acidic species with a $\text{pK}_a = -2$ while the protonated Py (PyH^+X^-) is weakly acidic with a $\text{pK}_a = 5.3$.²⁹ With the respect of the relative acid-base strength, it is envisaged that certain fractions of the Py terminals in TP-2Py will be protonated by the phenolic protons in PVPh, resulting in weakly (or non-) emissive protonated species responsible for the reduced emission observed in the TP-2Py/PVPh blend. Here emission efficiency of TP-2Py was considerably reduced by complexation to PVPh as indicated by Φ_F values of the solid samples (50 vs. 25%, Table 1). In contrast, little emission enhancement was observed in TP-2PTA system ($\Phi_F = 80$ and 85% for TP-2PTA and TP-2PTA/PVPh, respectively).

After recognizing that acidic phenolic function is harmful for the emission of

TP-2Py, neutral PVA was used to replace PVPh as the H-bond donating component. Unlike the acidic phenol groups in PVPh, the neutral hydroxyl groups of PVA should not protonate TP-2Py and produce no pyridinium species harmful for fluorescence. Indeed, the solid TP-2Py/PVA blend emit with stronger intensity than pure TP-2Py (Fig. 6A). Through steric constraint imposed by the polymer framework of PVA, molecular rotations of the pyridine and therefore the whole C2-substituents of TP-2Py can be effectively restricted, resulting in further emission enhancement of the AEE-active TP-2Py. The same result also holds for TP-2TPA as the corresponding emission spectrum (Fig. 6B) of the TP-2TPA/PVA blend is higher in emission intensity compared to pure TP-2TPA itself. The resultant Φ_F values of all solid blends (Table 1) are in line with the emission spectra shown in Fig. 5 and 6.

Experimental

Synthesis

Triphenylamine (TPA), phosphorous(v) oxychloride (POCl_3), triphenyl-methyl-phosphonium bromide ($\text{Ph}_3\text{PCH}_3\text{Br}$), potassium *tert*-butoxide (*t*-BuOK), bromine, Iron(III) chloride (FeCl_3), palladium(II) acetate ($\text{Pd}(\text{OAc})_2$), tri-*o*-tolylamine, sodium bicarbonate and 4-vinylpyridine (V-Py) were all purchased from Aldrich Chemical Co. and used directly without further purification. THF and DMF were refluxed over sodium and benzophenone under nitrogen for more than 2 days before distillation for use. Triethylamine (TEA) was distilled from CaH_2 under nitrogen before use. TP compound was prepared according to the reported procedures.^{26,27}

Preparation of 4-(diphenylamino)benzaldehyde(F-TPA). Triphenylamine (5g, 20.3mmol) was dissolved in 10 mL of DMF. POCl_3 (9.4 mL, 102 mmol) was

added drop to drop to the mixture at 0°C. After mixing, the temperature was raised to room temperature and during which, color of the solution turned red. The reaction mixture was then heated to 45°C and stirred for an additional 2 hr. The product mixture was poured in an ice-bath and neutralized with sodium bicarbonate. Recrystallization of resulting precipitates from ethanol. Pale yellow solid (5.4g, 96%) was collected by filtration. ¹H NMR (500MHz, d₆-DMSO): δ 9.79 (s, 1H, H_a), 7.7–7.75 (d, 2H, H_b), 7.4–7.5 (t, 4H, H_c), 7.15–7.25 (m, 6H, H_d), 6.85–6.9 (d, 2H, H_e) (Fig. S1); m/z (EI MS): calcd for C₁₉H₁₅NO, 273.12, found, 273.11; Anal calcd for C₁₉H₁₅NO: C, 83.49%; H, 5.53%; N, 5.12%, found: C, 83.47%; H, 5.54%; N, 5.13%.

Preparation of N,N-diphenyl-4-vinylaniline (V-TPA). To a solution of (9.8 g 27 mmol) of methyltriposponium bromide in 20 ml of THF (3.3 g, 29 mmol), potassium *tert*-butylate were added under cooling, during which the solution turned into yellow. The reaction solution was stirred for further 30 minutes and then (5 g, 18 mmol) of the 4-(diphenylamino)benzaldehyde (F-TPA) were added. The reaction was stirred for 24 hr at room temperature. The yellow solution was then extracted with methylene chloride. The product (3.7 g, 70%) was purified by column chromatography with toluene as eluent. ¹H NMR (500 MHz, d₆-DMSO): δ 6.89–7.4 (d, 14H, H_{d-h}), 6.61–6.7 (dd, 1H, H_b), 5.65–5.73 (d, 1H, H_c), 5.12–5.19 (d, 1H, H_a) (Fig. S2); m/z (EI MS): calcd for C₂₀H₁₇N, 271.14, found 271.10; Anal calcd for C₂₀H₁₇N: C, 88.59%; H, 6.31%; N, 5.1%, found: C, 88.52%; H, 6.34%; N, 5.14%.

Preparation of 2,5-bis(4-bromophenyl)-3,4-diphenylthiophene (TP-2Br). To a solution of 2,3,4,5-tetraphenylthiophene (5 g, 12.8 mmol) in 40 mL of CHCl₃ (40 mL) at 0 °C, ferric chloride (32 mg, 0.2 mmol) and bromine (4.2 g, 26.2 mmol) were added. This procedure was operated in the dark to avoid the undesired bromination on

the other portion of molecule. The solution was then warmed to room temperature before continuous reaction for 4 hr. The resultant slurry was poured into water and washed with sodium thiosulfate to the extent that the red color disappeared. The aqueous layer was extracted with CHCl_3 twice, and the combined organic layers were dried over magnesium sulfate. (5.1g, 83%). ^1H NMR (500 MHz, d_6 -DMSO): δ 6.97–6.99 (d, 4H, H_a), 7.12–7.18 (m, 10H, H_b), 7.47–7.48 (d, 4H, H_c) (Fig. S3); m/z (EI MS): calcd for $\text{C}_{28}\text{H}_{18}\text{Br}_2\text{S}$, 545.95, found, 545.93; Anal calcd for $\text{C}_{28}\text{H}_{18}\text{Br}_2\text{S}$: C, 61.57%; H, 3.32%. Found: C, 61.50%; H, 3.32%.

Preparation of

4,4'-((1E,1'E)-((3,4-diphenylthiophene-2,5-diyl)bis(4,1-phenylene))bis(ethene-2,1-diyl)dipyridine (TP-2Py). A reaction mixture of 4-vinylpyridine (1.1 mL, 10 mmol), TP-2Br (2.5 g, 4.58 mmol), triethylamine (30 mL), $\text{Pd}(\text{OAc})_2$ (0.33g, 1.47 mmol) and tri-*o*-tolylphosphine (0.22 g, 0.72 mmol) in dry DMF (30 mL) were placed in a predried round-bottomed flask (100 mL). The reaction mixture was then degassed by freeze–pump–thaw 3 times before heated at 110 °C for 24 hr. After cooling to room temperature, the reaction mixtures were poured into water to obtain yellow powder product. The crude product was then purified by flash column chromatography (v/v hexane/ethyl acetate = 4/1). (1.5g, 55%). ^1H NMR (500 MHz, d_6 -DMSO): δ 8.53 (d, 4H, H_a), 7.1–7.5 (m, 22H, H_{c-h}), 7.03 (d, 4H, H_b , $J_{trans} = 16.1$ Hz). ^{13}C NMR (500 MHz, d_6 -DMSO): δ 120.88, 126.55, 127.19, 127.27, 128.12, 128.91, 130.45, 132.16, 133.55, 135.46, 135.91, 137.58, 140.16, 144.17, 150.06 (Fig. S4); m/z (EI MS): calcd for $\text{C}_{42}\text{H}_{30}\text{N}_2\text{S}$, 594.21, found, 594.20; Anal calcd for $\text{C}_{42}\text{H}_{30}\text{N}_2\text{S}$: C, 84.9%; H, 5.09%; N, 4.71%, found: C, 84.83%; H, 5.14%; N, 4.72%.

Preparation of

4,4'-((1E,1'E)-((3,4-diphenylthiophene-2,5-diyl)bis(4,1-phenylene))bis(ethene-2,1-

diyl))bis(N,N-diphenylaniline) (TP-2TPA). A reaction mixture of V-TPA (2.12 g, 10 mmol), TP-2Br (2.5 g, 4.58 mmol), triethylamine (30 mL), Pd(OAc)₂ (0.33 g, 1.47 mmol) and tri-*o*-tolylphosphine (0.22 g, 0.72 mmol) in dry DMF (30 mL) were placed in a predried round-bottomed flask (100 mL). The reaction mixture was then degassed by freeze–pump–thaw 3 times before heated at 110 °C for 24 hr. After cooling to room temperature, the reaction mixtures were poured into water to obtain yellow powder products. The crude products were then purified by flash column chromatography (v/v hexane/ethyl acetate = 4/1). (2.5g, 58.8 %). ¹H NMR (500 MHz, d₆-DMSO): δ 7.02–7.47 (m, 46H, H_{b-i}). 6.93–6.94 (d, 4H, H_a, *J*_{trans}=16.3 Hz). ¹³C NMR (500 MHz, d₆-DMSO): δ 122.91, 123.35, 124.21, 125.95, 126.39, 127.09, 127.70, 128.07, 128.51, 128.80, 129.62, 130.47, 131.18, 132.24, 136.07, 136.61, 137.56, 139.78 (Fig. S5); m/z (EI MS): calcd for C₆₈H₅₀N₂S, 926.37, found, 926.35; Anal Calcd for C₆₈H₅₀N₂S: C, 88.17%; H, 5.44%; N, 3.02%, found: C, 88.2%; H, 5.4%; N, 3.1%.

Instrumentations

The emission spectra were obtained from a LabGuide X350 FL spectrophotometer using a 450W Xe lamp as the continuous light source. Temperature-programming PL emission spectra were conducted using a Peltier cell from Ocean Optics connecting to HCS 302 hot stage. Quantum yield (Φ_F) of the solid sample was measured in an integrating sphere made by Ocean Optics. For liquid solutions, value of Φ_{PL} was obtained by using quinine sulfate as reference standard. The UV-vis absorption spectra were recorded with an Ocean Optics DT 1000 CE 376 spectrophotometer. To measure the solution UV-Vis absorption and emission spectra, quartz cell with dimensions of 0.2 x 1.0 x 4.5 cm³ was used. Stock solutions of the fluorophores were primarily prepared and aliquot of the stock solution was transferred to 10 mL volumetric flask, into which appropriate volumes of hexane and THF was added

dropwise under vigorous stirring to furnish solution with desired concentration and hexane content. Particle sizes of fluorophores and fluorophore/polymer mixtures in different solvent media were measured by DLS instrument on a Malvern ZetaSizer Nano ZS90 spectrometer at room temperature. A He–Ne laser operating at 633 nm was used as light source. Fluorophore/polymer blends were prepared from mixing the respective components in THF solvent. Mixing was conducted by vigorous stirring till precipitation occurred. Solid samples were prepared by dropping the solution over quartz plate to obtain solid specimen for measurement. ^1H NMR spectra were recorded with a Varian VXR-500 MHz FT-NMR instrument. Tetramethylsilane was used as internal standard. Elemental analyses were performed on an Elementary Vario EL-III C, H and N analyzer. A mass spectrum was obtained by using a Bruker Daltonics Autoflex III MALDI-TOF mass spectrometer.

Conclusion

TP-2Py and TP-2PTA with TP center connected by the respective Py and TPA terminals were successfully synthesized from the Heck-coupling reactions between TP2Br and the corresponding diene monomers. The resultant TP-2Py and TP-2PTA were found to exhibit AEE fluorescence behavior that the solution fluorescence intensity increases with increasing aggregation upon adding hexane poor solvent in the solution mixtures. With the large TPA terminals, TP-2PTA has higher solution and solid emission intensities than TP-2Py under the same experimental conditions. Therefore, the large TPA terminals in TP-2PTA imposed effective rotational restriction, rendering in high emission efficiency (e.g. solid TP-2PTA has a high Φ_F of 80%). In contrast, less effective rotational restriction of TP-2Py resulted in a lower emission efficiency (e.g. solid TP-2Py has a Φ_F of 50%) than TP-2PTA.

Theoretically, H-bonding to polymers will further enhance fluorescence of TP-2Py and TP-2PTA because that molecular rotation of the fluorophores can be hampered by the viscous polymeric segments in close vicinities. However, the alkaline TP-2Py tends to react with the acidic phenol groups in PVPh, resulting in protonated species with reduced emission intensity compared to TP-2Py itself. The acid-base reaction can be avoided by using neutral PVA instead; therefore, further emission enhancement was observed in TP-2Py/PVA blend. For TP-2PTA, complexation to PVPh and PVA all resulted in further emission enhancements because the neutral TPA terminals can be immune from acid-base reaction. The idea using H-bond interaction to enhance emission of AEE-active fluorophores was therefore demonstrated in this study.

Acknowledgement

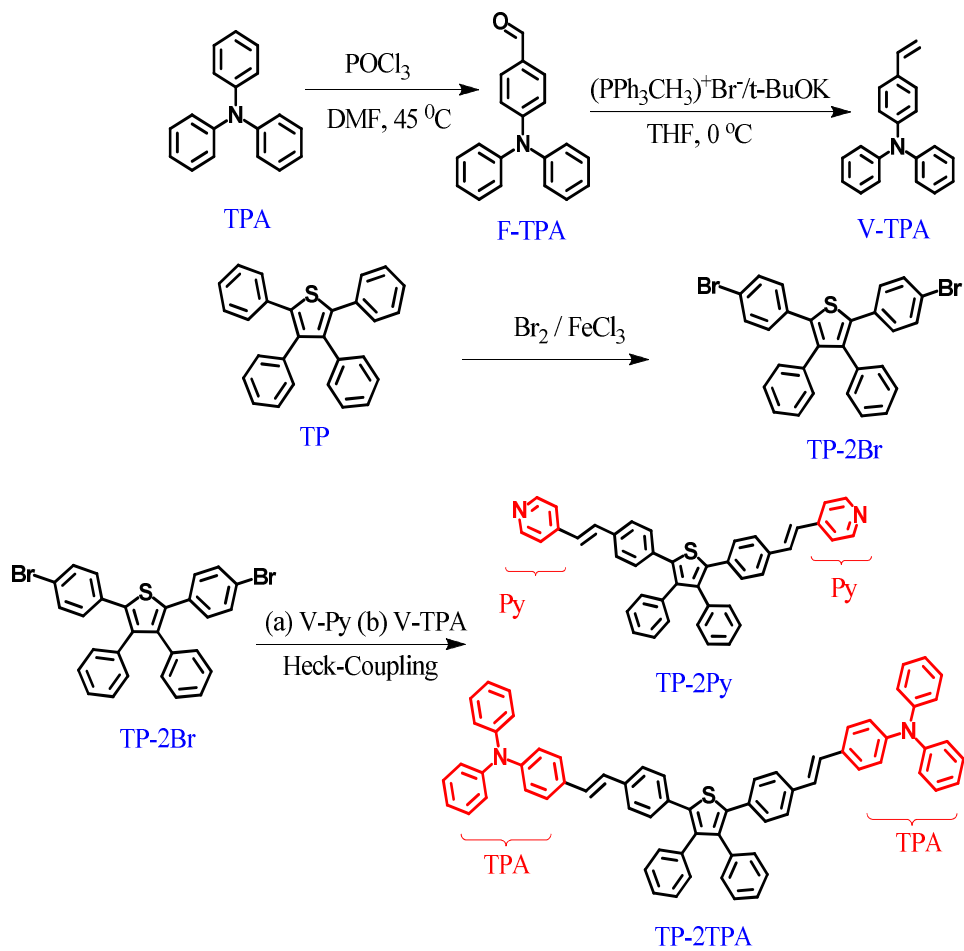
We appreciate the financial support from National Science Council, Taiwan, under the contract no. NSC 102-2221-E-110-084-MY3

References

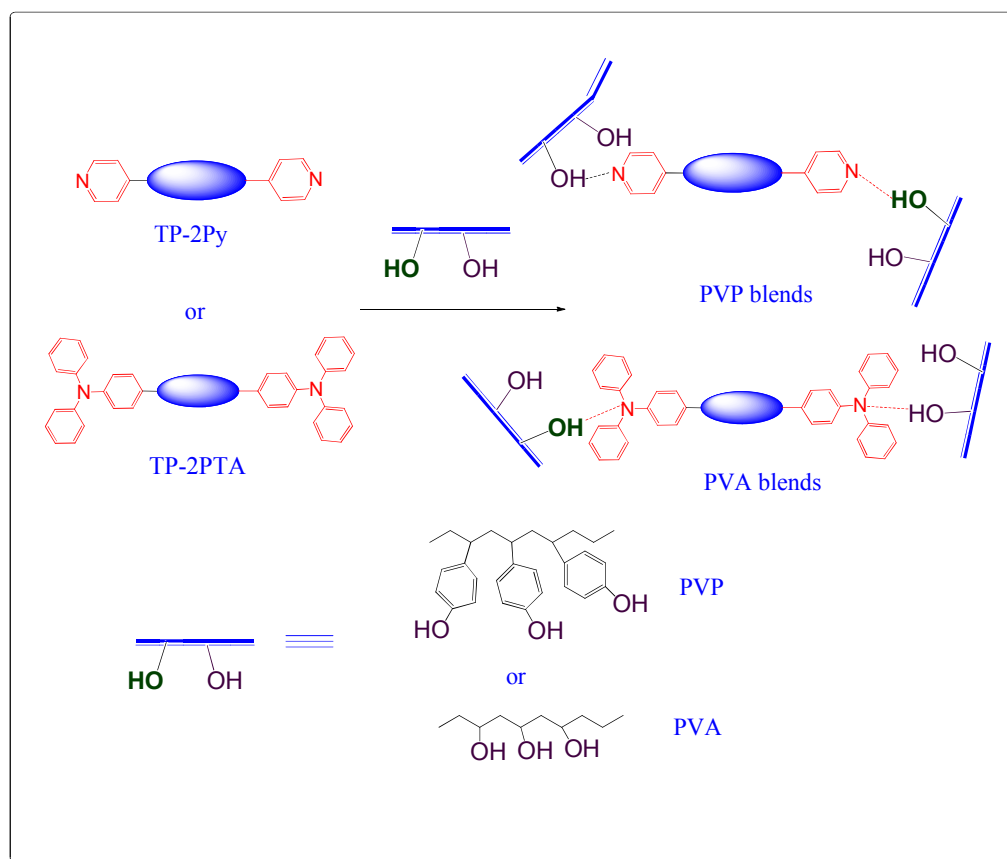
- 1 J. Luo, Z. Xie, J. W. Y. Lam, L. Cheng, H. Chen, C. Qiu, H. S. Kwok, X. Zhan, Y. Liu, D. Zhu and B. Z. Tang, *Chem. Commun.*, 2001, 1740.
- 2 H. Y. Chen, W. Y. Lam, J. D. Luo, Y. L. Ho, B. Z. Tang, D. B. Zhu, M. Wong and H. S. Kwok, *Appl. Phys. Lett.*, 2002, **81**, 574.
- 3 J. Chen, C. C. W. Law, J. W. Y. Lam, Y. Dong, S. M. F. Lo, I. D. Williams, D. Zhu and B. Z. Tang, *Chem. Mater.*, 2003, **15**, 1535.
- 4 J. Chen, Z. Xie, J. W. Y. Lam, C. C. W. Law and B. Z. Tang, *Macromolecules*, 2003, **36**, 1108.
- 5 J. Chen, H. Peng, C. C. W. Law, Y. Dong, J. W. Y. Lam, I. D. Williams and B. Z.

- Tang, *Macromolecules*, 2003, **36**, 4319.
6. Z. Zhao, S. Chen, J. W. Y. Lam, C. K. W. Jim, C. Y. K. Chan, Z. Wang, P. Lu, C. Deng, H. Kwok, Y. Ma and B. Z. Tang, *J. Phys. Chem. C*, 2010, **114**, 7963.
7. W. Z. Yuan, X. Y. Shen, H. Zhao, J. C. W. Lam, L. Tang, P. Lu, C. Wang, Y. Liu, Z. Wang, Q. Zheng, J. Z. Sun, Y. Ma and B. Z. Tang, *J. Phys. Chem. C* 2010, **114**, 6090.
8. Y. Hong, J. W. Y. Lam and B. Z. Tang, *Chem. Commun.*, 2009, 4332.
9. J. Liu, J. W. Y. Lam and B. Z. Tang, *J. Inorg. Organomet. Polym.*, 2009, **19**, 249.
10. J. Wu, W. Liu, J. Ge, H. Zhang and P. Wang, *Chem. Soc. Rev.*, 2011, **40**, 3483.
11. Y. Hong, J. W. Y. Lam and B. Z. Tang, *Chem. Soc. Rev.*, 2011, **40**, 5361.
12. A. Qin, J. W. Y. Lam and B. Z. Tang, *Prog. Polym. Sci.*, 2012, **37**, 182.
13. Z. Zhao, J. W. Y. Lam and B. Z. Tang, *Soft Matter*, 2013, **9**, 4564.
14. J. Huang, X. Yang, X. Li, P. Chen, R. Tang, F. Li, P. Lu, Y. Ma, L. Wang, J. Qin, Q. Li and Z. Li, *Chem. Commun.*, 2012, **48**, 9586.
15. J. Huang, N. Sun, Y. Dong, R. Tang, P. Lu, P. Cai, Q. Li, D. Ma, J. Qin and Z. Li, *Advanced functional Materials* 2013, **18**, 2329.
16. Y. Liu, X. Tao, F. Wang, J. Shi, J. Sun, W. Yu, Y. Ren, D. Zou and M. Jiang, *J. Phys. Chem. C*, 2007, **111**, 6544.
17. P. Chen, R. Lu, P. Xue, T. Xu, G. Chen and Y. Zhao, *Langmuir*, 2009, **25**, 8395.
18. P. Zhang, H. Wang, H. Liu and M. Li, *Langmuir*, 2010, **26**, 10183.
19. H. Kim, M. S. Choi, B. H. Sohn, S. Y. Park, W. S. Lyoo and T. S. Lee, *Chem. Commun.*, 2008, 2364.
20. J. H. Wan, L. Y. Mao, Y. B. Li, Z. F. Li, H. Y. Qiu, C. Wang and G. Q. Lai, *Soft Matter*, 2010, **6**, 3195.
21. M. K. Nayak, *J. Photochem. Photobiol., A*, 2011, **217**, 40.
22. R. H. Chien, C. T. Lai and J. L. Hong, *J. Phys. Chem. C*, 2011, **115**, 12358.

- 23 R. H. Chien, C. T. Lai and J. L. Hong, *J. Phys. Chem. C*, 2011, **115**, 20732.
- 24 W. L. Chien, C. M. Yang, T. L. Chen, S. T. Li and J. L. Hong, *RSC Adv.*, 2013, **3**, 6930.
- 25 J. T. Lai and J. L. Hong, *J. Phys. Chem. B*, 2010, **114**, 10302.
- 26 A. Pourjavadi, M. R. Zamanlu, and M. J. Zohyriaan-Mehr, *J. Appl. Polym. Sci.* 2000, **77**, 1144.
- 27 Y. Imai, N. N. Maldar, and M. Kakimoto, *J. Polym. Sci., Polym. Chem.*, 1984, **22**, 2189.
- 28 B. Valeur, *Molecular Fluorescence, Principles and Applications*, page 36, Wiley-VCH, Weinheim, Germany, 2002, page 36.
- 29 N. Thomas, *Organic Chemistry*, Sorrell University Science Book, 2006, page 152.



Scheme 1 Syntheses of AEE-active fluorophores of TP-2Py and TP-2TPA.



Scheme 2 Blends of TP-2Py and TP-2PTA with poly(vinyl phenol) (PVPh) and poly(vinyl alcohol) (PVA) through H-bond interaction.

Table 1 Quantum yield (Φ_F)^a of solid TP-2Py, TP-2TPA and their complexes with PVPh and PVA.

sample	TP-2Py	TP2TPA	TP-2Py/ PVPh blend	TP-2Py/ PVA blend	TP-2TPA/ PVPh blend	TP2TPA/ PVA blend
Φ_F , %	50	80	25	54	85	84

^a quantum yield was obtained from integrating sphere.

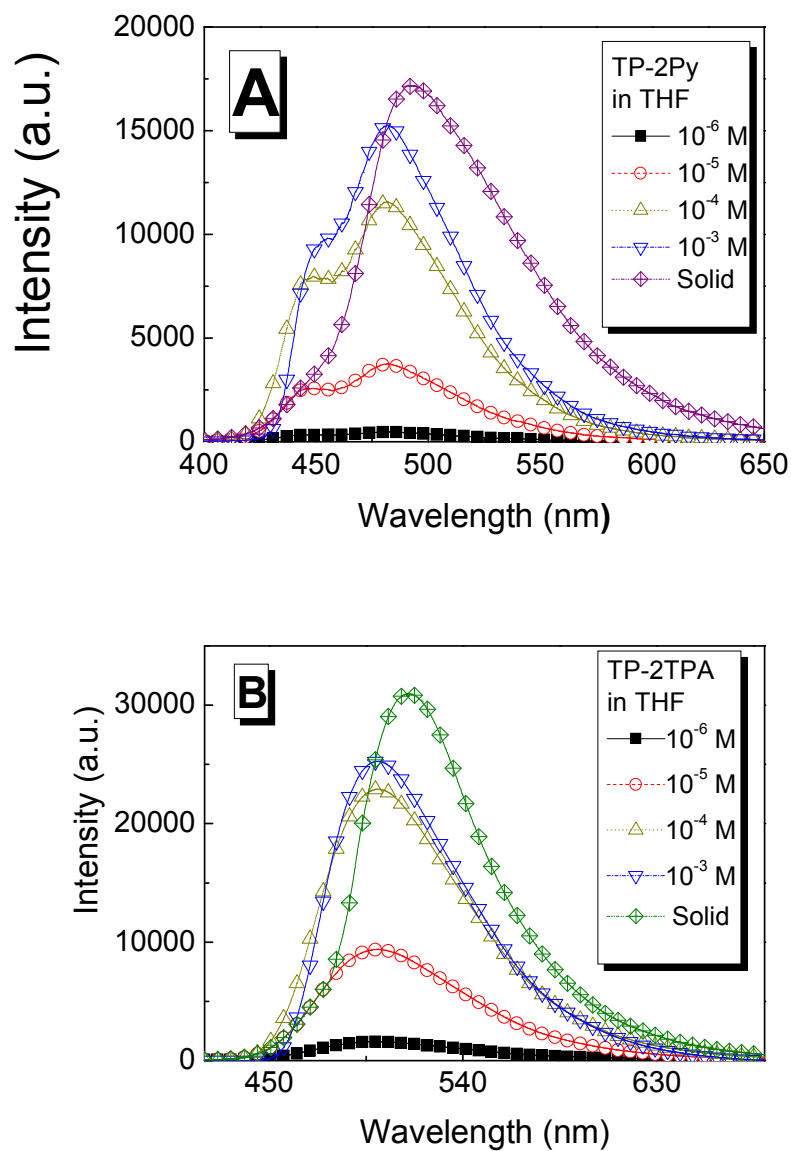


Fig. 1 Solution PL emission spectra of (A) TP-2Py and (B) TP-2PTA in THF of different concentrations. ($\lambda_{\text{ex}} = 365$ nm for TP-2Py and 390 nm for TP-2PTA)

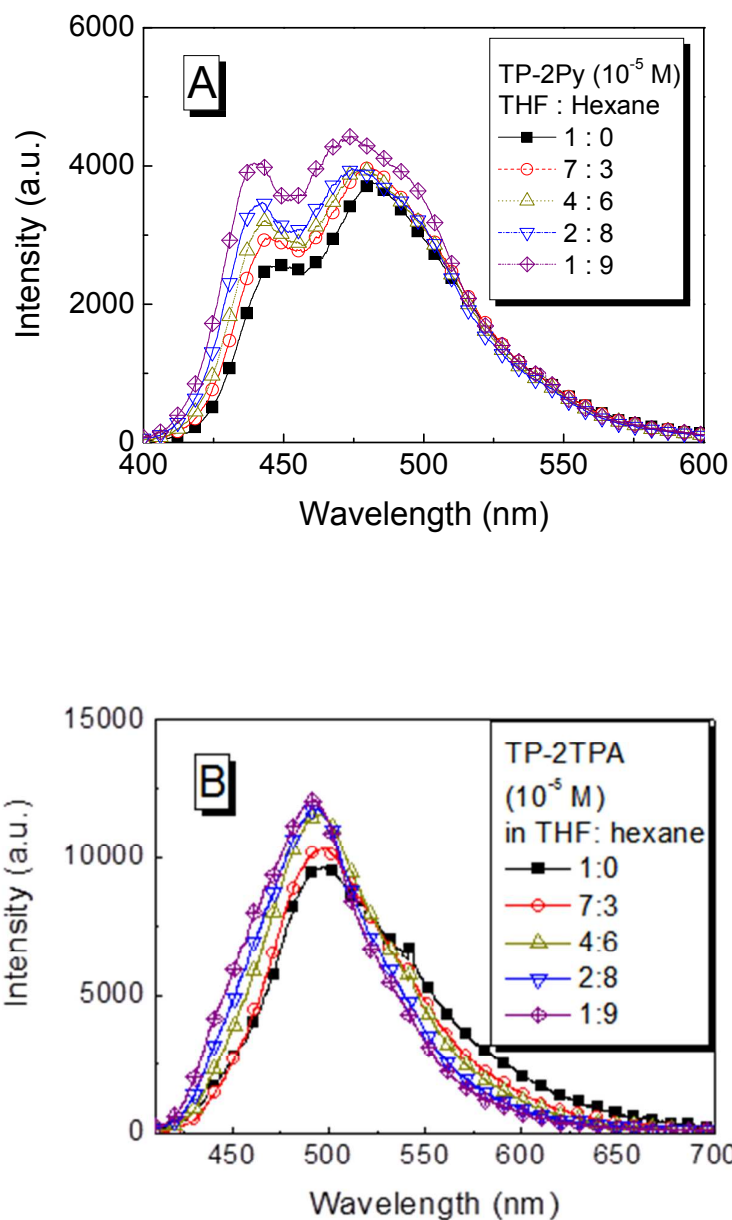


Fig. 2 Solution PL emission spectra of (A) TP-2Py and (B) TP-2PTA in THF/hexane mixtures of different volume ratios. ($\lambda_{\text{ex}} = 365$ nm for TP-2Py and 390 nm for TP-2PTA)

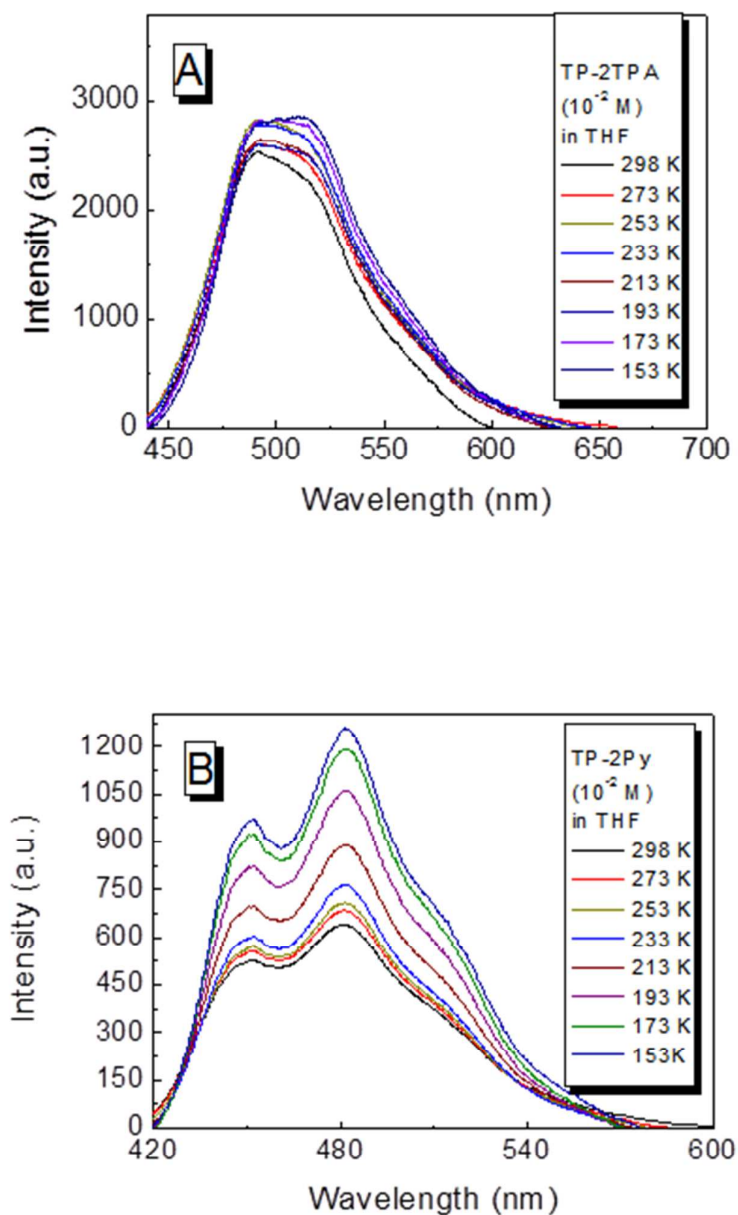


Fig. 3 Solution PL emission spectra of (A) TPA-2Py and (B) TP-2PTA in THF (10^{-2} M) at different reduced temperatures from 298 to 153 K. ($\lambda_{\text{ex}} = 365$ nm for TP-2Py and 390 nm for TP-2PTA)

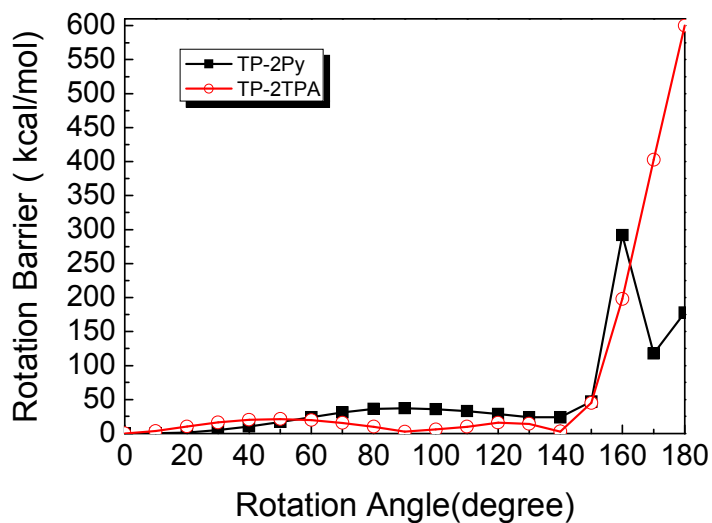
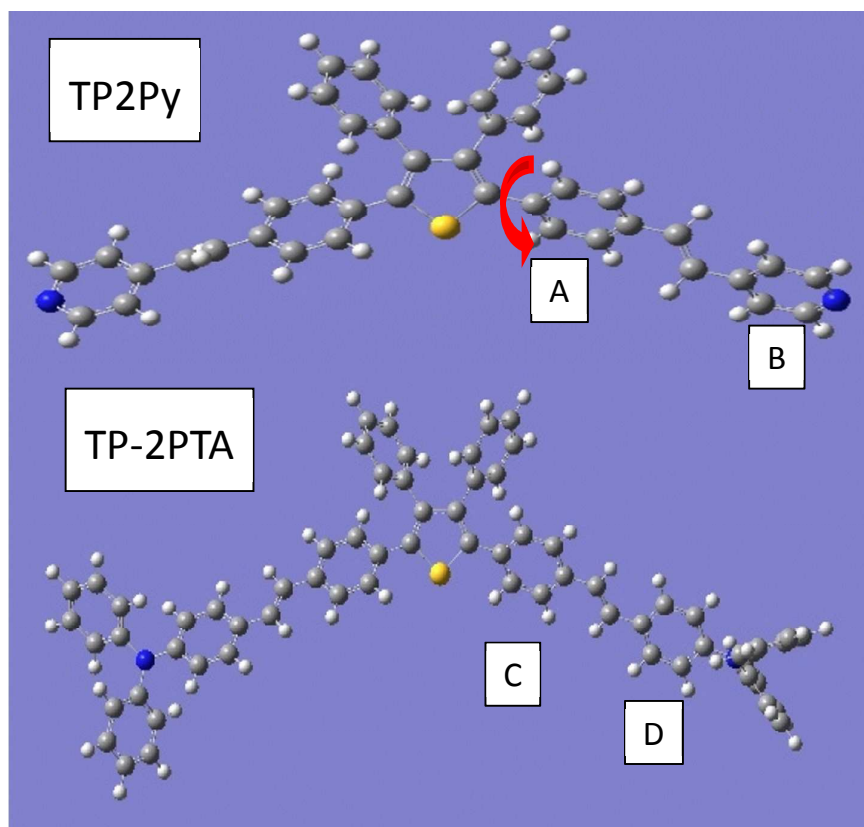


Fig. 4 The simulated conformers (top) of TP-2Py and TP-2PTA with minimum energy and the calculated rotation energy barriers versus rotation angle (bottom).

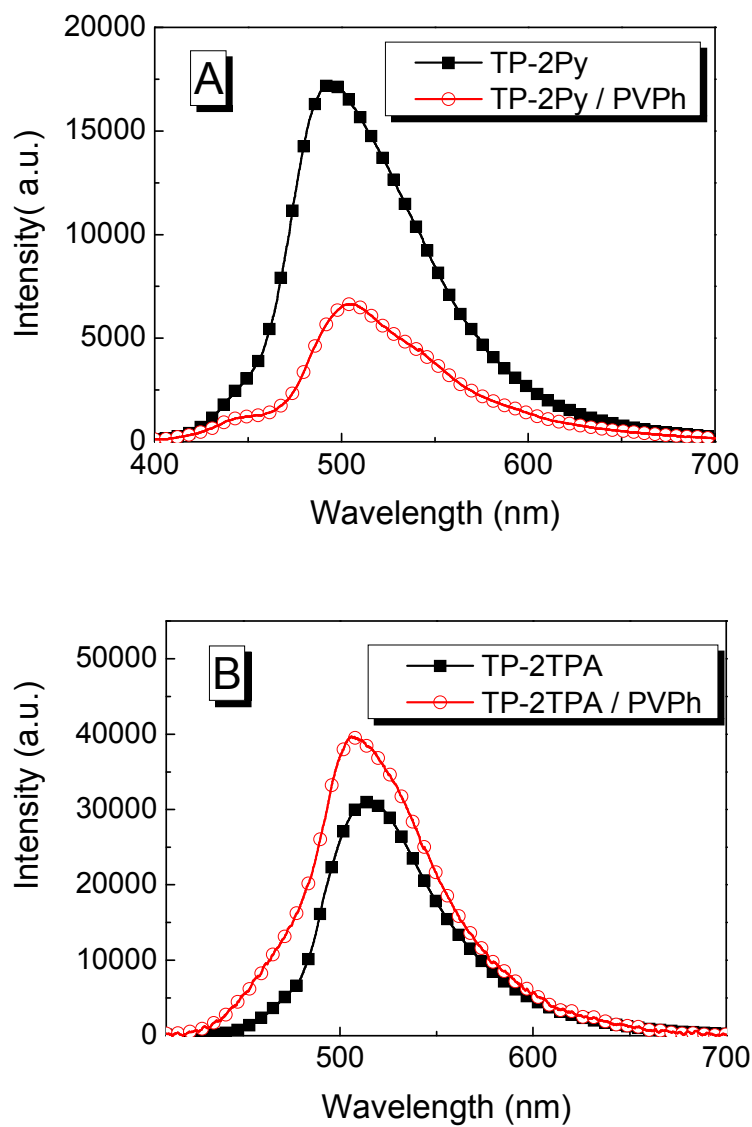


Fig. 5 The solid PL emission spectra of (A) TP-2Py and TP-2Py/PVPh blend and (B) TP-2PTA and TP-2PTA/PVPh blend. ($\lambda_{\text{ex}} = 365$ nm for TP-2Py system and 390 nm for TP-2PTA system)

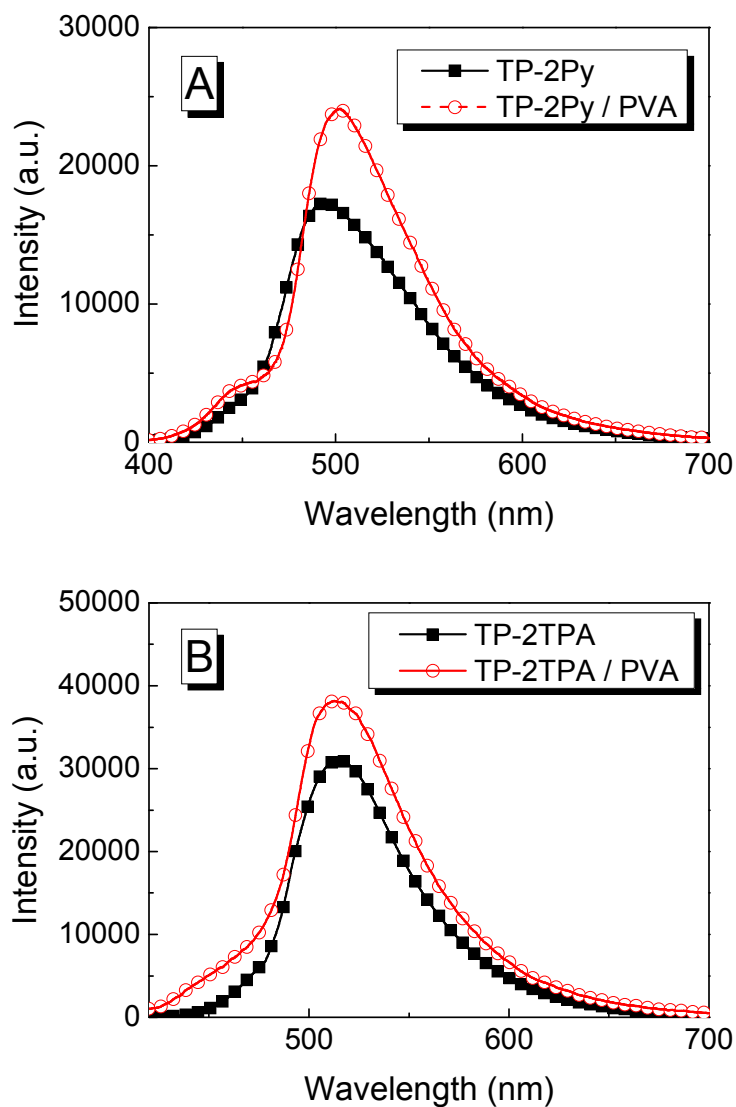


Fig. 6 The solid PL emission spectra of (A) TP-2Py and TP-2Py/PVA blend and (B) TP-2PTA and TP-2PTA/PVA blend. ($\lambda_{\text{ex}} = 365$ nm for TP-2Py system and 390 nm for TP-2PTA system)

Content of TOC